RESEARCH ARTICLE

Functional genomic profiling of *Aspergillus fumigatus* biofilm reveals enhanced production of the mycotoxin gliotoxin

Sandra Bruns[1,2], Marc Seidler[3]*, Daniela Albrecht[4], Stefanie Salvenmoser[3], Nicole Remme[5], Christian Hertweck[5], Axel A. Brakhage[1,2], Olaf Kniemeyer[1,2]** and Frank-Michael C. Müller[3]*

[1] Department of Molecular and Applied Microbiology, Hans-Knöll-Institute, Jena, Germany
[2] Department of Microbiology and Molecular Biology, Friedrich Schiller University Jena, Jena, Germany
[3] Pediatric Pulmonology and Infectious Diseases, Department of Pediatrics, University Heidelberg, Heidelberg, Germany
[4] Research Group Systems Biology/Bioinformatics, Hans-Knöll-Institute, Jena, Germany
[5] Department of Biomolecular Chemistry, Leibniz Institute for Natural Product Research and Infection Biology, Hans-Knöll-Institute, Jena, Germany

Received: March 1, 2010
Revised: June 1, 2010
Accepted: June 5, 2010

The opportunistic pathogenic mold *Aspergillus fumigatus* is an increasing cause of morbidity and mortality in immunocompromized and in part immunocompetent patients. *A. fumigatus* can grow in multicellular communities by the formation of a hyphal network encased in an extracellular matrix. Here, we describe the proteome and transcriptome of planktonic- and biofilm-grown *A. fumigatus* mycelium after 24 and 48 h. A biofilm- and time-dependent regulation of many proteins and genes of the primary metabolism indicates a developmental stage of the young biofilm at 24 h, which demands energy. At a matured biofilm phase, metabolic activity seems to be reduced. However, genes, which code for hydrophobins, and proteins involved in the biosynthesis of secondary metabolites were significantly upregulated. In particular, proteins of the gliotoxin secondary metabolite gene cluster were induced in biofilm cultures. This was confirmed by real-time PCR and by detection of this immunologically active mycotoxin in culture supernatants using HPLC analysis. The enhanced production of gliotoxin by *in vitro* formed biofilms reported here may also play a significant role under *in vivo* conditions. It may confer *A. fumigatus* protection from the host immune system and also enable its survival and persistence in chronic lung infections such as aspergilloma.

Keywords:
2-D gel electrophoresis / *Aspergillus fumigatus* / Biofilm / Gliotoxin / Microarrays / Microbiology

1 Introduction

Aspergillus fumigatus is a prevalent opportunistic fungal pathogen especially in immunocompromized and partly in immunocompetent individuals. It has the ability to filament within the lungs forming dense intertwined mycelial balls [1]. The virulence of *A. fumigatus* is caused by proteins that promote mycelia growth into the lung parenchyma and by structural features of the conidia that confer resistance to the host antifungal defense mechanisms [2, 3]. Moreover, *A. fumigatus* can produce immunosuppressive toxins such as gliotoxin that may enable it to persist in the respiratory tract [4].

Correspondence: Professor Frank-Michael C. Müller, Pediatric Pulmonology and Infectious Diseases, Department of Pediatrics, University Heidelberg, Im Neuenheimer Feld 430, 69120 Heidelberg, Germany
E-mail: frank-michael_mueller@med.uni-heidelberg.de
Fax: +49-6221-56-33853

Abbreviations: ATP, adenosine triphosphate; **ECM,** extracellular matrix; **FDH,** formate dehydrogenase; **FunCat,** Functional Catalogue; **NAD,** nicotinamide adenine dinucleotide; **RT-PCR,** real-time PCR

*These authors have contributed equally to this work.
**Additional corresponding author: Dr. Olaf Kniemeyer
E-mail: olaf.kniemeyer@hki-jena.de

In their natural environments, most bacterial and fungal species are able to shift between a planktonic and a sessile (biofilm) state [5]. Among fungi, biofilm formation has been studied most intensively in the pathogenic yeast *Candida albicans* (reviewed in [6]). However, several research groups have investigated the capacity of *A. fumigatus* to form a biofilm. The fungus was shown to produce a parallel-packed hyphal network on plastic surfaces or bronchial epithelial cells embedded in an extracellular matrix (ECM) [7–9]. A first proof for *in vivo* formation of biofilms was recently reported in patients with aspergilloma [10]. Since *A. fumigatus* biofilm formation seems to be clinically relevant, it is of major importance to analyze its molecular basis in chronic lung infections such as aspergilloma. Still an open question is whether a special gene expression program needs to be initiated and new proteins are synthesized for a sessile growth of *A. fumigatus*. Here, we provide the first comprehensive profiling and analysis of the proteome and transcriptome of planktonic and biofilm-grown *A. fumigatus* mycelium after 24 and 48 h by applying a recently established *in vitro* biofilm model [9]. Our results suggest a decrease in metabolic activity (respiration) during biofilm maturation, an upregulation of proteins and genes of the sulfur metabolism, oxidative stress response and several surface proteins of the hydrophobin class. Most strikingly, an increased production of the mycotoxin gliotoxin in *A. fumigatus* cultures grown as biofilm was observed. Our data imply that gliotoxin may be a putative factor for *A. fumigatus* to persist in chronic lung infections.

2 Materials and methods

2.1 Fungal strains and culture conditions

A conidial solution of *A. fumigatus* ATCC ♯46645 was prepared, cultured on coated flasks for 24 and 48 h of both planktonic and biofilm growth as described previously [9]. Two different media were inoculated with a final concentration of 10^6 conidia/mL: The medium for biofilm formation was MEM with 5% v/v FCS. The control medium was MEM with 5% v/v PBS. Serum was added to the biofilm media because it stimulates the growth of a dense hyphal network. Cultures were incubated at 37°C and 5% CO_2 for 2 h to let the fungus adhere to the surface. To remove nonattached conidia, the culture was washed, new MEM (containing FCS or PBS) was added and the fungus was left to produce biofilm for 24 and 48 h.

2.2 Protein isolation

After 24/48 h of biofilm or planktonic growth, *A. fumigatus* mycelium was collected and washed twice by filtering through Miracloth (MSD, Germany) with PBS to remove FCS. The mycelium was frozen by liquid nitrogen and grounded in a precooled mortar. An aliquot of 100 mg mycelium was dispersed in 500 μL cold extraction buffer and proteins were purified by the phenol extraction methanol/ammonium acetate precipitation method described in [11]. Protein pellets were dried for 5 min at room temperature and dissolved in 2-D gel electrophoresis lysis buffer as described in [12, 13]. Protein concentration was determined with Bradford reagent (Bio-Rad, Germany).

2.3 2-D PAGE

For DIGE, the pH of the samples was adjusted to 8.5 with 100 mM NaOH. Afterward, the samples were labeled with CyDye minimal dyes according to the protocol of GE Healthcare as described in [12]. An internal standard of 25 μg protein of every sample (control and biofilm) was pooled, labeled with Cy2 (dissolved in DMF) and used on all gels. In total, 50 μg of control and biofilm protein extracts were labeled with 300 pmol of either Cy3 or Cy5 fluorescent dyes. IPG strip equilibration and SDS-gel electrophoresis were performed as described in [13]. The proteins were visualized with a Typhoon 9410 scanner using a resolution of 100 μm. For spot picking, proteins were visualized by colloidal Coomassie staining [14] or by ruthenium II *tris*(bathophenanthroline disulfonate) as described in [15].

For statistical reproducibility, we applied an extended loop design using three biological replicates in dye swap (Cy3 and Cy5) and a global internal standard (Cy2) consisting of a pool of all 12 samples. The following samples were loaded on a gel in triplicate: 24 h biofilm with 24 h planktonic growth, 48 h biofilm with 48 h planktonic growth, 24 h with 48 h biofilm growth and 24 h with 48 h planktonic growth.

2.4 Detection of spots and matching of gels

Detection of spots and matching of gels were achieved using DeCyder™ v6.5 software. Background subtracted data were exported and further analyzed using R and Bioconductor. Normalization and filtering were conducted as described previously [16]. Application of the robust *Z*-Score on confidence level 99% resulted in a fold change threshold of 1.9. Above this threshold, protein spots were regarded as being differentially regulated. For statistical significance, two-way ANOVA was applied to the normalized data. Two-way ANOVA assesses both experimental factors (time and growth type) separately and can therefore filter out which of the factors have contributed to the significance of a certain protein spot. Additionally, it analyzes the interaction of both factors resulting in low *p*-values when both factors play a role in the regulation of a spot. In all three ANOVA analyses (one-way time, one-way growth type and two-way interaction of time and growth type), protein spots were regarded as

being statistically significant when the respective *p*-value (false discovery rate corrected for multiple testing) was below 0.05. Differentially expressed proteins were analyzed by MALDI-TOF/TOF.

2.5 MS identification

Proteins were identified on a Bruker Ultraflex I MALDI-TOF/TOF device (Bruker Daltonics, Germany) operating in reflectron mode as summarized in Supporting Information Table S8 and [17].

2.6 RNA isolation

Total RNA was isolated from biofilm- and planktonic-grown mycelium in three independent experiments using TRI Reagent (Sigma-Aldrich, Germany). Isolated RNA was treated with DNase I (Invitrogen, Germany) and further purified with RNeasy Clean up columns (Qiagen, Germany). The RNA's quality and quantity were checked using Agilent Total RNA Nano 6000 chips (Agilent, Germany). cDNA was synthesized from 1.5 μg of total RNA using the First Strand cDNA kit (Roche, Germany). Additionally, we analyzed two types of controls. Instead of culturing in an incubator with CO_2, we incubated 48 h biofilm in normal air under the same conditions to check for a possible influence of CO_2. The second control was performed using vigorous shaking at 220 rpm using the same conditions of 48 h biofilm growth to avoid the production of a biofilm due to lack of attachment.

2.7 Microarray analysis

Arrays were obtained from the J. Craig Venter Institute (TIGR, Rockville, IN, USA) as an unrestricted grant. The RNA of 24 and 48 h planktonic- and biofilm-grown *A. fumigatus* was extracted using the methods described above. Briefly, 20 μg pure RNA of each condition was synthesized using the LabelStar Array Kit (Qiagen) with aadUTP (Sigma-Aldrich) instead of aadTTP. As washing buffer, a TRIS-free buffer containing 84.25 mL 95% v/v ethanol, 15.25 mL H_2O and 0.5 mL 1 M $KHPO_4$ was used. The dried pellets were resuspended in 4.5 μL 0.1 M $NaHCO_3$. After 1 h of incubation at room temperature with 4.5 μL Cy-dye esters (GE Healthcare, Germany) in DMSO, the probes were neutralized with 35 μL 100 mM NaOAc (pH 5.1) and incubated for 15 min with 4.5 μL hydroxylamine at room temperature. The cleanup was performed using the Qiaquick PCR Purification Kit (Qiagen). For stabilization, 5 μg poly(A)-DNA (MWG Biotech, Germany), 10 μg Cot1 DNA (Roche) and 20 μg yeast tRNA (Sigma-Aldrich) were added and the pellets dried in a SpeedVac. The hybridization of the arrays was performed according to the protocol of TIGR (SOP#M008 http://pga.tigr.org). The chips were scanned and analyzed using an Axon GenePix 4000B scanner and the GenePix4 software. Only those spots were used for analysis, which were regulated similarly on each array in both dye swap conditions.

Log2 ratios of normalized spot intensities were filtered for differential regulation using *Z*-Scores and ANOVA. All intensity signals with a log2 ratio outside the range of ± 2.3 at 24 h and of ± 4 at 48 h were regarded as being differentially regulated based on a confidence interval of 95%.

2.8 Real-time PCR

After 2-D gel and microarray analysis, the expression profiles of five different genes were confirmed by real-time PCR (RT-PCR). For quantification and normalization, β-actin was used as a housekeeping gene. RT-PCR was performed with the Roche LightCycler apparatus using LightCycler Fast Start Master SYBR Green (Roche). The PCR reactions were performed at 60–62°C and elongation time ranked from 12 to 15 s. The specificity of the RT-PCR was controlled by leaving out the template or the reverse transcriptase. As additional controls, the formation of biofilm was triggered by different methods, *e.g. A. fumigatus* nonbiofilm +/− shaking by 220 rpm and +/− CO_2, to avoid the possibility of false results due to the condition of biofilm production.

Specific primers (Supporting Information Table S1) were designed using the full-length sequence from the NCBI database. A standard curve of amplification efficiency of each gene was generated from purified PCR products across five orders of magnitude dilution series. Samples were analyzed in duplicates and for aberrance from more than half a cycle, the experiment was repeated.

2.9 Analysis of gliotoxins by HPLC and LC-MS

Supernatants of cell cultures were extracted three times with 100 mL of ethyl acetate. The combined organic phases were dried over sodium sulfate, evaporated and redissolved in 800 μL methanol. Samples were measured on a Jasco HPLC with DAD and on a LC-Q ES-MS from Thermo Electron, respectively. Gliotoxin standard was received from Sigma-Aldrich and a calibration curve was established from 16 μg to 1 mg gliotoxin.

For HPLC measurements, 20 μL of the concentrated sample were injected (Column: Nucleosil 100 (250×4.6 mm, C_{18} 5 μM). Eluent: 1 mL/min flow, isocratic, A: H_2O, 0.1% v/v TFA, B: ACN; for 30 min 40% v/v B, 10 min 100% B). For LC-MS measurements, 25 μL of the concentrated sample were injected (Column: Nucleosil 100 (250×4.6 mm, C_{18} 5 μM) Eluent: 0.6 mL/min flow, gradient, A: H_2O, 0.1% HCOOH, B: ACN; start 20% B, in 18 min 65% B, after 28 min 95% B for 10 min). Gliotoxin eluted

from the HPLC column after 6.4 min and from the LC-MS-column after 17.3 min.

2.10 Confocal laser scanning microscopy

Confocal laser scanning microscopy of biofilm-grown *A. fumigatus* was performed as described previously [9].

2.11 Statistical analysis

The statistical significance of differences between groups was assessed by false discovery rate corrected two-way ANOVA using R and Bioconductor. Results were considered significant at $p < 0.05$.

2.12 Data deposition

The microarray data reported in this article have been deposited in the GeneExpressionOmnibus database, www.ncbi.nlm.nih.gov/geo (accession no. GSE19430). Additionally, microarray and 2-D gel data are publicly available at OmniFung, a data warehouse for integrating fungal ''omics'' data, www.omnifung.hki-jena.de.

3 Results and discussion

3.1 Global study of the biofilm development of *A. fumigatus* by whole genome DNA chips and proteome analysis

There is very little information available on the proteome changes during biofilm development in *Aspergillus* species [18]. Due to technical limitations, *in vivo*-grown *A. fumigatus* biofilms from patients are hardly accessible for global gene and protein expression profiling. To get a comprehensive picture of the molecular basis of *A. fumigatus* biofilm formation, we analyzed the proteome and transcriptome of *A. fumigatus* mycelium grown planktonically or as biofilm. RNA and protein samples were taken after 24 and 48 h, so that an intermediate and mature developmental status of the *A. fumigatus* biofilm could be compared (Supporting Information Fig. S1).

The expression of several proteins changed significantly in biofilm-grown mycelium (Fig. 1). The abundance of 36 protein spots changed in biofilm mycelium of *A. fumigatus* in comparison to planktonic mycelium (planktonic *versus* biofilm). Briefly, 78 protein spots changed significantly during the maturation of the biofilm (24 *versus* 48 h). In total, 35 protein spots showed significant changes depending on both the time (24 *versus* 48 h) and the growth condition (planktonic *versus* biofilm). Altogether, 33 different proteins were identified by MALDI-TOF/TOF-analyses

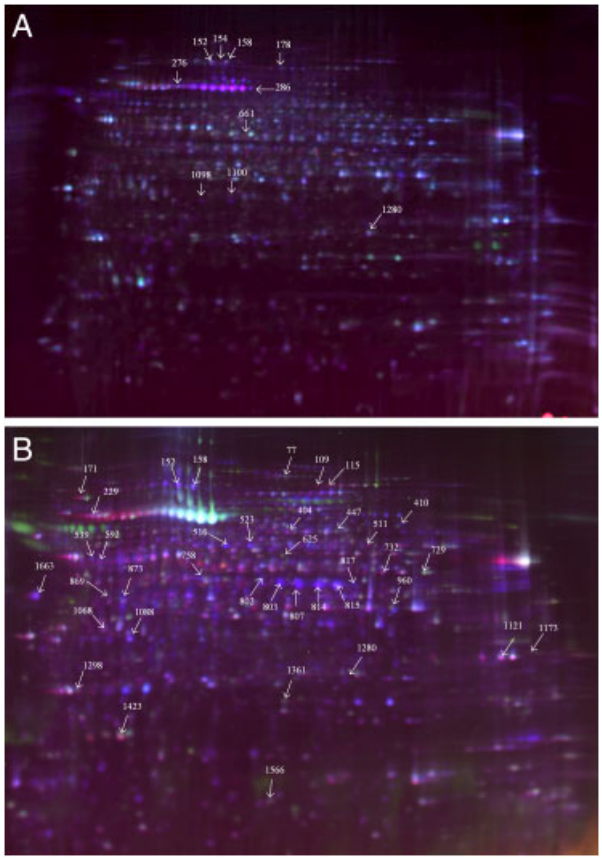

Figure 1. 2-D gel electrophoresis of protein extracts stained with the DIGE-labeling technique. The orientation of the IEF is indicated. The numbers refer to proteins whose levels changed significantly. (A) Comparison of biofilm protein extracts after 24 h (Cy3-red) and planktonic protein extracts after 24 h (Cy5-blue); (B) Protein extracts of 24 h (Cy5-blue) and 48 h (Cy3-red) biofilms.

(Table 1, Fig. 1 and Supporting Information Table S8). The protein expression of enzymes of the catabolic carbohydrate, amino acid and secondary metabolism as well as proteins involved in protein processing altered most significantly. In addition, identified proteins were subjected to Functional Catalogue (FunCat) classification [19]. Most identified proteins, differentially expressed in biofilm in comparison to planktonic cultures, belonged to the first level FunCat categories ''metabolism'', ''protein with binding function or cofactor requirement'' and ''cellular transport, transport facilitation and transport routes''. A comparison of the protein expression over time in biofilm cultures revealed a quite similar picture (Figs. 2A and B).

During comparison of the transcriptional profile of planktonic- and biofilm-grown mycelium cultivated for 24 h, 740 genes were differentially regulated (179 up and 561 downregulated), whereas in 48 h biofilms a total number of 687 genes showed differential expression (569 up and 118 downregulated). Totally, 143 genes were differently

Table 1. Biofilm- (biofilm *versus* planktonic grown) and time-dependent (48 *versus* 24 h), differentially synthesized proteins of *A. fumigatus*

Putative function	Fold change[a)]			
	Biofilm-dependent chances		Time-dependent changes in biofilm	
	24+/24−	48+/48−	48+/24+	48−/24−
Glycolysis, pyruvate metabolism				
960 Glyceraldehyde 3-phosphate-DH (AFUA_5G01970)	n.s.	n.s.	−3.2	−0.9
404 Pyruvate decarboxylase PdcA (AFUA_3G11070)	n.s.	n.s.	−3.4	0.4
516 Aldehyde dehydrogenase AldA (AFUA_6G11430)	n.s.	n.s.	4.0	0.9
523 ''–''	n.s.	n.s.	2.2	0.6
539 Enolase/allergen Asp F22 (AFUA_6G06770)	n.s.	n.s.	2.1	0.7
Citric acid cycle				
77 α-Ketoglutarate DH, subunit Kgd1 (AFUA_4G11650)	n.s.	n.s.	−2.6	−1.4
178 Mitochondrial aconitase (AFUA_6G12930)	2.1	0.4	n.s.	n.s.
729 Citrate synthase Cit1 (AFUA_5G4230)	n.s.	n.s.	−2.4	−1.2
732 ''–''	n.s.	n.s.	−2.3	−1.2
Respiration and oxidative phosphorylation				
229 ATP synthase F1, β-subunit (AFUA_5G10550)	n.s.	n.s.	0.9	2.5
410 ATP synthase F1, α-subunit (AFUA_8G05320)	n.s.	n.s.	−2.4	−2.6
511 ''–''	n.s.	n.s.	−2.3	−0.9
869 Inorganic diphosphatase (AFUA_3G08380)	n.s.	n.s.	2.7	1.3
873 ''–''	n.s.	n.s.	2.7	1.3
1068 ''–''	n.s.	n.s.	5.2	1.7
1361 ATP synthase D chain (AFUA_6G03810)	n.s.	n.s.	−2.0	−1.3
Formate catabolic process				
803 NAD-dependent formate DH (AFUA_6G04920)	n.s.	n.s.	13.0	2.7
807 ''–''	n.s.	n.s.	11.4	3.1
814 ''–''	n.s.	n.s.	34.0	2.9
815 ''–''	n.s.	n.s.	20.7	2.5
817 ''–''	n.s.	n.s.	3.2	0.9
Ergosterol biosynthesis				
625 Hydroxymethylglutaryl-CoA synthase Erg13 (AFUA_3G10660)	n.s.	n.s.	−2.1	−1.3
Protein and amino acid metabolism, processing				
152 Secreted dipeptidyl peptidase (AFUA_2G09030)	0.8	1.9	3.5	1.7
154 Methionine synthase MetH/D (AFUA_4G07360)	2.3	6.6	n.s.	n.s.
158 ''–''	n.s.	n.s.	1.8	2.7
592 Mitochondrial peptidase, β-subunit (AFUA_1G14200)	n.s.	n.s.	2.3	1.8
661 Glutamate/Leucine/Penylalanine/Valine-DH (AFUA_4G06620)	−2.2	−12.2	n.s.	n.s.
758 *S*-adenosylmethionine synthetase (AFUA_1G10630)	n.s.	n.s.	2.9	1.0
1663 Aspartic endopeptidase Pep2 (AFUA_3G11400)	n.s.	n.s.	4.0	1.5
Translation				
109 Translation elongation factor EF-2 (AFUA_2G13530)	n.s.	n.s.	−5.7	−2.6
115 ''–''	n.s.	n.s.	−3.5	−0.5
1121 40S ribosomal protein S3 (AFUA_1G05630)	n.s.	n.s.	−2.3	−0.5
Stress response, protein folding				
171 Molecular chaperone Hsp90/Hsp1 (AFUA_5G04170)	n.s.	n.s.	−4.1	−1.7
276 Mitochondrial chaperone Ssc70 (AFUA_2G09960)	1.6	2.1	n.s.	n.s.
286 HSP70 chaperone HscA (AFUA_8G03990)	1.8	2.3	n.s.	n.s.
1423 Allergen AspF3 (AFUA_6G022880)	n.s.	n.s.	−3.0	−1.1
Signal transduction/translational control				
802 G-protein complex CpcB, β-subunit (AFUA_4G13170)	n.s.	n.s.	6.1	1.1
Secondary metabolism				
1088 Thioredoxin reductase GliT (AFUA_6G09740)	n.s.	n.s.	2.1	1.2
1098 Phytanoyl-CoA dioxygenase family protein (AFUA_8G00230)	1.8	3.4	n.s.	n.s.
1100 ''–''	5.6	6.1	n.s.	n.s.
1280 Glutathione *S*-transferase GliG (AFUA_6G09690)	n.s.	n.s.	3.5	1.1
Others				
447 UTP-glucose-1-phosphate uridylyltransferase (AFUA_7G01830)	n.s.	n.s.	−1.9	−0.7
1173 Outer mitochondrial membrane protein porin (AFUA_4G06910)	n.s.	n.s.	−2.2	−0.8
1298 Conserved protein AFUA_5G14680	−2.1	1.5	3.4	1.1

+, biofilm growth; −, planktonic growth; n.s., no significant fold change.

a) Average ratios extracted from statistical analysis of DIGE-gels by the Decyder 6.5 software (BVA analysis) and subsequent imputation and normalization of protein abundance values.

expressed at both time points (Supporting Information Fig. S2). To get more detailed information about specific gene expression, differentially expressed genes were classified according to first level FunCat terms (Figs. 2C and D). Many upregulated genes were involved in protein synthesis, metabolism, energy conservation and encoded for proteins with binding function or cofactor requirement, whereas many downregulated genes were involved in signal transduction, cell type differentiation, interaction with the environment, biogenesis of cellular components, regulation of metabolism and protein function as well as cell and protein fate (Supporting Information Tables S2a and S2b). In addition, significantly enriched second level FunCat terms were identified for the positively and negatively regulated genes in biofilm mycelium in comparison to planktonic mycelium after 24 and 48 h (Supporting Information Tables S3 and S4). Obviously, biofilm growth induces a conspicuous genetic reprogramming. First, the transcriptional regulation of genes involved in cellular signaling and stress response is modified. For example, several components of the mitogen-activated protein kinase signaling (*mpkB* and *mpkC*) and cAMP signal transduction pathway (*gpaB* and *ganA*) showed a lower expression in the biofilm culture as well as genes coding for proteasome

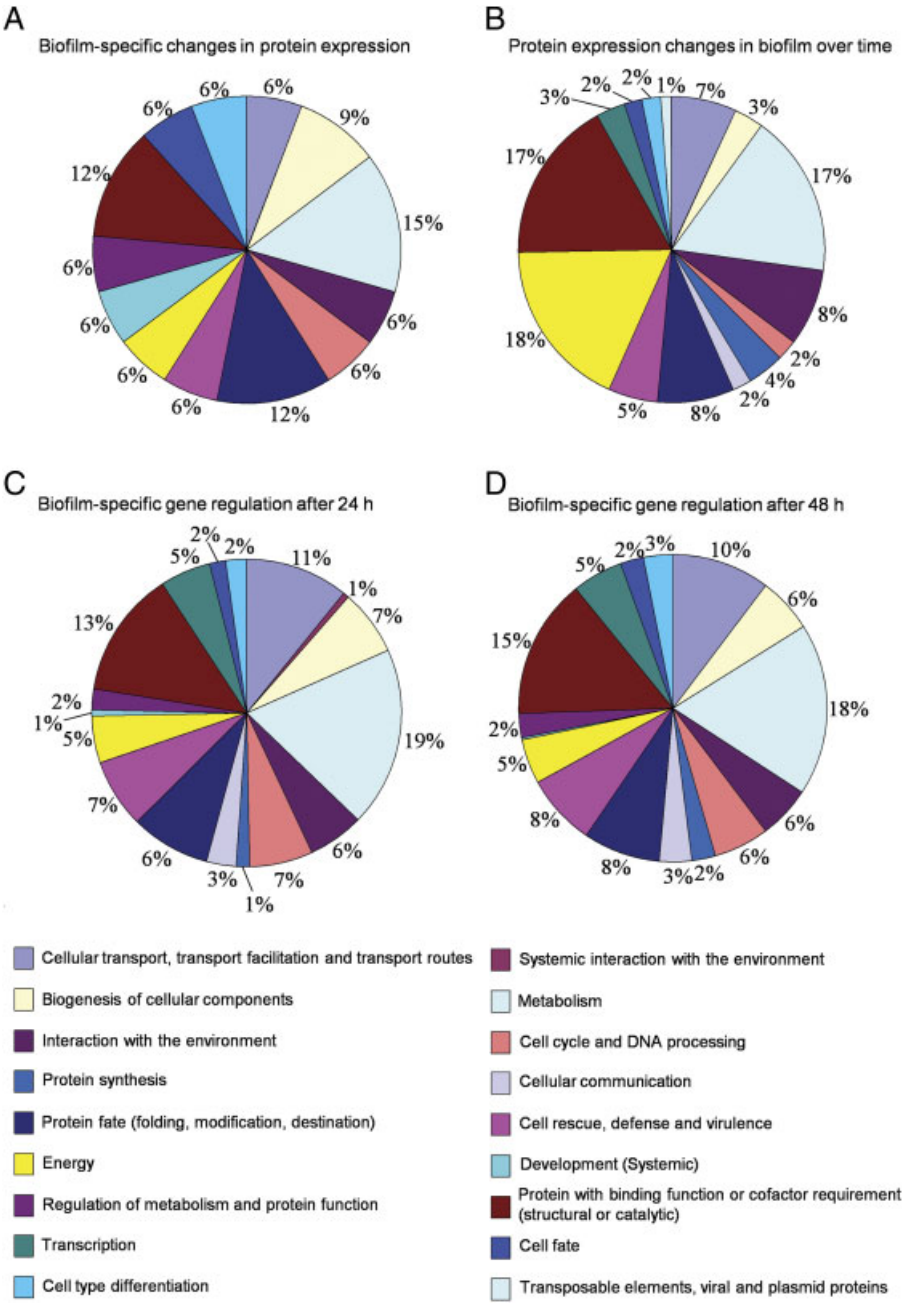

Figure 2. First level FunCat classification of differently expressed proteins in biofilm-grown *A. fumigatus* cultures (thresholds, see Section 2.4). (A) Changes of biofilm cultures in comparison to planktonic-grown cultures and (B) changes in biofilm-grown cultures over time (comparison of 24 h culture *versus* 48 h biofilm culture). First level FunCat classification of significantly regulated genes in biofilm-grown *A. fumigatus* cultures in comparison to planktonic-grown cultures (thresholds, see Section 2.7). (C) 24 h planktonic *versus* biofilm growth and (D) 48 h planktonic *versus* biofilm growth.

components. Later, in mature biofilms, the cellular metabolism undergoes significant changes. Thus, several genes putatively involved in the biosynthesis of secondary metabolites showed increased expression, whereas several genes coding for hypothetical proteins or amino acid metabolism enzymes (lysine and asparagine) were downregulated.

3.2 Gene and protein expression analysis of the basic carbohydrate and amino acid metabolism

On the proteome level, proteins involved in amino acid biosynthesis, protein degradation and the tricarboxylic acid (TCA)-cycle showed a differential regulation in biofilm-grown mycelium. During biofilm maturation (24 *versus* 48 h), the level of enzymes of the glycolysis, citric acid cycle adenosine triphosphate (ATP) synthesis decreased over time, whereas an aldehyde dehydrogenase was significantly upregulated. A nicotinamide adenine dinucleotide (NAD)-dependent formate dehydrogenase (FDH) was one of the most highly upregulated proteins over time (Fig. 3). The corresponding gene showed a biofilm- and time-dependent regulation too. The functional role of FDH in fungi has not been elucidated in detail yet [20, 21]. In plants, FDH is significantly induced under low-oxygen partial pressure and other stress-inducing conditions, when the NAD^+/NADH ratio is unbalanced [22, 23]. In *A. fumigatus*, a similar induction is conceivable, but has not been described yet and the specific biological role of FDH has to be further investigated. Furthermore, our microarray analysis revealed an upregulation of the alcohol dehydrogenases and further genes of the ethanol metabolism (AFUA_3G11070, AFUA_5G6240, and AFUA_7G01000) in biofilm-grown cultures after 48 h. It is interesting to speculate that the upregulated alcohol dehydrogenases may be involved in generating quorum-sensing aryl- and acyl-alcohol and hence regulating biofilm formation, as it has been reported for *Candida* [24]. Until now, nothing is known about putative quorum-sensing molecules in *A. fumigatus*, but it is conceivable that they exist in filamentous fungi.

Taken together, these data indicate a developmental stage of the biofilm at 24 h that demands energy, whereas at a more mature phase of the biofilm metabolic activity seems to be reprogrammed. This is also in good agreement with a previously reported reduction of metabolic activities in mature biofilms in *Candida* [25] and may also explain, at least in part, the higher resistance of *A. fumigatus* biofilm-grown cultures against antifungal drugs [7, 9, 26]. *C. albicans* and *A. fumigatus* also share common regulation patterns of the sulfur metabolism during biofilm growth [26–28]. A methionine synthase and *S*-adenosylmethionine synthetase (AFUA_1G10630) demonstrated an increased level over time in sessile mycelium, whereas the transcript of *S*-adenosylmethionine synthetase was slightly upregulated after 24 h biofilm, but downregulated in 48 h biofilm (Fig. 3). Similarly, the expression of the putative sulfur metabolism regulator gene *skpA* was significantly increased in mature biofilm (48 h). It was speculated for *C. albicans* that biofilms have a special requirement for methionine and cysteine-rich proteins, which may also hold true for *A. fumigatus*.

3.3 Antigens, stress and drug resistance

The transcriptome data reveal that among known IgE-binding allergens, Asp f1, Asp f2, Asp f4 and Asp f13 were upregulated (Fig. 3) in a time-dependent manner (AFUA_5G02330, AFUA_4G09580, AFUA_2G03830 and AFUA_2G12630). It seems that the allergens are secreted simultaneously with the production of the ECM. This may also explain the upregulation of many genes of the vacuolar transport. The highly upregulated gene coding for Cu, Zn and superoxide dismutase (AFUA_5G9240) has also been shown to be immunoreactive [29]. The superoxide dismutase that detoxifies superoxide anions, the main precursor of ROS, could putatively confer resistance to *A. fumigatus* biofilms from ROS during growth and persistence in the host. By contrast, transcript levels of the Mn superoxide dismutase (AFUA_1G14550) decreased significantly in biofilms. Furthermore, many major facilitator superfamily and ATP-binding cassette transporters were slightly upregulated in a time-dependent manner (Fig. 3). The major facilitator superfamily and ATP-binding cassette transporters are known to influence the development of antibiotic resistance. This indicates that with the onset of the production of the ECM antifungal drug resistance may occur [9].

3.4 Cell wall and surface proteins

In the genome of *A. fumigatus*, six different putative hydrophobin proteins have been identified. These cysteine-rich proteins are present only in filamentous fungi and are known to form hydrophobic surface layers on conidia and hyphal walls [7, 30]. Analysis of the transcriptome data revealed upregulation of genes coding for several hydrophobins (rodlet proteins). Although *rodD* (AFUA_5G01490) was upregulated at 24 h biofilm, *rodB* (AFUA_1G17250), *rodC* (AFUA_8G07060) and *rodE* (AFUA_8G05890) were upregulated in 48 h biofilm (Fig. 3). Interestingly, in a recent study, only *rodB* and *rodE* were found to be expressed in static, aerial grown hyphae which resembles biofilm-like growth [7]. The biological role of the hydrophobin-like proteins RodD, RodC and RodE has not been elucidated yet, but it is conceivable that they are involved in the formation of the ECM and thus may mediate surface adhesion and hamper immune recognition as reported for the conidial hydrophobin RodA [30].

In addition, several cell wall genes were highly expressed in *A. fumigatus* biofilm, *e.g.* a chitin synthase

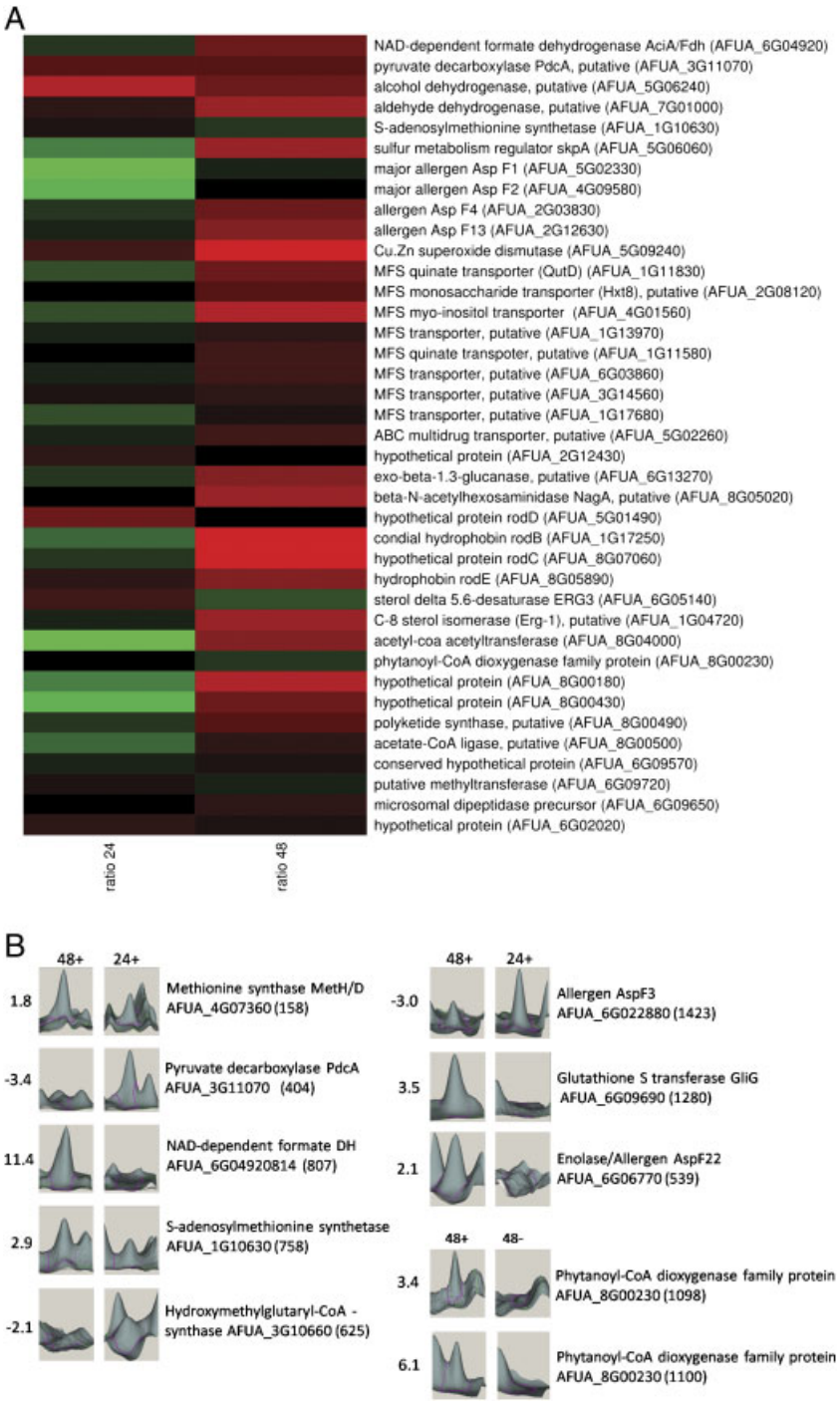

Figure 3. (A) Heatmap of selected genes which were upregulated in *A. fumigatus* during biofilm growth. Red color shows up and green color downregulation (from –9 to +11). (B) 3-D view of the selected protein spots that showed a change in abundance during biofilm development or in comparison to planktonically grown mycelium of *A. fumigatus*.

(AFUA_2G13430), a β-1,3-glucanase (AFUA_6G13270) or the β-*N*-acetylhexosaminidase gene *nagA* (AFUA_8G05020). The β-glucan pathway may restructure the biofilm cell wall and/or may also be involved in the production of extracellular polymeric matrix as discussed for *C. albicans* [31].

Transcriptional changes were also observed for genes implicated in the maintenance of the membrane fluidity (Fig. 3). Three genes involved in the biosynthesis of ergosterol were upregulated. In 24 h biofilm, *erg3* (AFUA_6G05140) and in 48 h biofilm *erg1* (AFUA_1G04720) and *erg10* (AFUA_8G04000) were significantly expressed at a higher level in comparison to the planktonic-grown cultures. *Erg1* is the target of the antifungal drug terbinafine that confers resistance, if substituted [32]. *Erg10* is involved in germ tube formation. The

increased level of *erg* genes may explain the observed higher resistance of *A. fumigatus* biofilms to antifungal compounds that target the ergosterol biosynthesis pathway.

3.5 Secondary metabolism

A. fumigatus is able to produce a wide range of natural products, in the form of secondary metabolites, some of which are determinants of virulence. Interestingly, several genes or proteins, which are involved in the biosynthesis of secondary metabolites, were upregulated in biofilm-grown cultures of *A. fumigatus* (Fig. 3, Table 1, Supporting Information Tables S4 and S5).

Proteome and transcriptome analysis revealed that enzymes or genes, which are part of the fumitremorgin supercluster, showed a biofilm-dependent change in expression [33]: a phytanoyl-CoA dioxygenase family protein (AFUA_8G00230) and the genes AFUA_8G00180, AFUA_8G00430, AFUA_8G00490 and AFUA_8G00500.

Additionally, in proteome and transcriptome studies, genes and proteins involved in the biosynthesis of the mycotoxin gliotoxin (cluster comprises the genes AFUA_6G09580 to AFUA_6G09770) were upregulated in biofilm-grown cultures as well. The putative glutathione *S*-transferase GliG showed a 3.5-fold increased protein level in biofilm-grown mycelium after 48 h and the putative thioredoxin reductase GliT showed a 2.1-fold increased level over time. After 24 h of biofilm growth, the gliotoxin genes *gliN* (AFUA_6G09720) and *gliT* (AFUA_6G09740) were induced by approximately twofold, whereas after 48 h the transcript levels of *gliJ* (AFUA_6G09650) and the putative aldehyde reductase *gliO* (AFUA_5G02020), which is not part of the gliotoxin cluster, increased more than twofold.

Gliotoxin is a small, hydrophobic nonribosomal dipeptide that exerts toxic effects on phagocytic cells and T-lymphocytes at low concentrations *in vitro*. It is discussed as a virulence factor in invasive aspergillosis by suppressing the innate and adaptive immune response [34].

3.6 Comparison of transcriptome and proteome data

A comparison of our transcriptome with the proteome data revealed only very low similarities (Supporting Information Table S7). For genes and their corresponding proteins of the protein and amino acid metabolism, a relatively good correlation was found (protein spot nos. 152, 154 and 661), but for others, such as heat shock proteins (protein spot nos. 276 and 286) the regulation was reverse. Low correlation of the expression of mRNA and the abundance of corresponding proteins has also been reported in other studies of *A. fumigatus* [35]. Several reasons for this miscorrelation are discussed, such as different *in vivo* half lives of mRNA and proteins, post-transcriptional regulation on the protein level and the technical errors caused by the different analysis techniques, *e.g.* 2-D gel electrophoresis is limited in the detection of membrane and very hydrophobic proteins [36].

3.7 Confirmation of transcriptome and proteome data by RT-PCR

To verify the upregulation of the gliotoxin gene cluster in a mature *A. fumigatus* biofilm grown for 48 h, four genes were analyzed by quantitative RT-PCR. The following genes were selected: the NRPS gene *gliP* (key enzyme not detected in transcriptome and proteome analysis), *gliG* (detected in the proteome), *gliN* (upregulated gene in biofilm) and *gliT* (upregulation on the proteome and transcript level). The β-actin gene *act1* was used as housekeeping control. The results for 48 h biofilm formation against planktonic growth showed a significant change of the expression profile (Supporting Information Table S6).

The gene *gliN* showed a fourfold upregulation in biofilm compared with planktonic-grown *Aspergillus* cultures, the expression of *gliG* increased 12 fold and *gliT* 31 fold in biofilm-grown cells. As additional controls, 48 h biofilm, *e.g.* nonbiofilm +/− shaking by 220 rpm and +/− CO_2 was performed to exclude the influence of CO_2 and vigorous shaking on the gliotoxin production rate. The results showed more or less the same expression pattern. Transcripts of *gliP* were not detected in this experiment, possibly due to their size and their relatively low abundance in

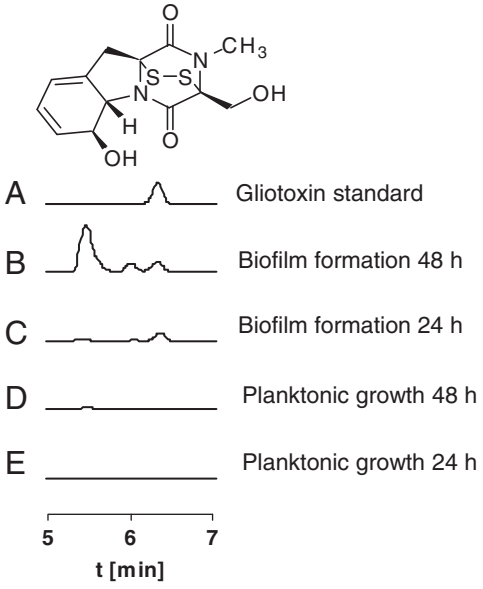

Figure 4. Detection of gliotoxin in culture supernatants by HPLC. Gliotoxin eluted after 6.4 min as revealed by the injection of standard gliotoxin (A). Supernatants of biofilm-grown cultures harvested after 48 h (B) and 24 h (C) were analyzed. Planktonic-grown cultures were used as control (D and E).

comparison to the other genes of the cluster. Presumably by reason of limited dynamic range of microarray expression measurements and different probe design, the fold change of gene expression did not exactly correlate with the RT-PCR data [37].

3.8 Analysis of gliotoxin content in culture supernatants

To verify the proteome and transcriptome data, the amount of gliotoxin in the supernatant of cultures grown for 24 and 48 h as biofilm or in shaking flasks was quantified by HPLC. In biofilm-grown cultures, the gliotoxin concentration increased from 0.75 mg/L culture broth at 24 to 1.2 mg/L after 48 h. In the supernatants of planktonic-grown mycelium and all controls, no or just traces of gliotoxin were detected (Fig. 4). To confirm the results of the HPLC analysis, extracts of culture supernatants were also analyzed by LC-Q ES-MS and compared with a gliotoxin standard. Mass fragmentation of *m/z* 327 resulted in the typical major fragment ions *m/z* 263 and 245 [38].

4 Concluding remarks

A. fumigatus possesses the classical elements of biofilm growth (sessile and matrix production), but genes or proteins specifically involved in this process have not been described up to now. Here, we provide the first comprehensive study of the molecular basis of biofilm formation in *A. fumigatus*. Several unexpected observations were made, including the high expression of hydrophobin genes and, most interestingly, the formation of several secondary metabolites including gliotoxin, which could help the fungus to protect from the immune system during chronic lung infection. The observation that gliotoxin biosynthesis genes were induced during initiation of murine infection in *A. fumigatus* is consistent with our model that gliotoxin may be of importance for the persistence of noninvasive, but chronic infections [39]. Gliotoxin has modulatory effects on the host's immune system ([38], reviewed in [40]). Growing as a multicellular community and producing gliotoxin and other secondary metabolites may alleviate *A. fumigatus* survival especially in the immunocompetent host, for instance in cystic fibrosis patients with chronic lung infections, patients with allergic bronchopulmonary aspergillosis, aspergilloma or sinusitis [41].

The microarray data reported in this article have been deposited in the GeneExpressionOmnibus (GEO) database, www.ncbi.nlm.nih.gov/geo (accession no. GSE19430). Additionally, microarray and 2-D gel data are publicly available at OmniFung, a data warehouse for integrating fungal "omics" data, www.omnifung.hki-jena.de.

This work was supported by the Deutsche Forschungsgemeinschaft (Priority Program 1160) to A. A. B., and the HKI. The A. fumigatus microarrays were obtained from J. Craig Venter Institute (TIGR) (Rockville, USA) as an unrestricted grant to F.-M. C. M. The authors are grateful to Silke Steinbach and Maria Pötsch as well as Robert Winkler for assistance in proteome analysis and MS analysis, respectively. Svenja Simon is acknowledged for generating heat maps.

The authors have declared no conflict of interest.

5 References

[1] Mowat, E., Williams, C., Jones, B., McChlery, S., Ramage, G., The characteristics of *Aspergillus fumigatus* mycetoma development: is this a biofilm? *Med. Mycol.* 2008, *47*, 1–7.

[2] Brakhage, A. A., Systemic fungal infections caused by *Aspergillus* species: epidemiology, infection process and virulence determinants. *Curr. Drug Targets* 2005, *6*, 875–886.

[3] Askew, D. S., *Aspergillus fumigatus*: virulence genes in a street-smart mold. *Curr. Opin. Microbiol.* 2008, *11*, 331–337.

[4] Sugui, J. A., Pardo, J., Chang, Y. C., Mullbacher, A. *et al.*, Role of *laeA* in the regulation of *alb1*, *gliP*, conidial morphology, and virulence in *Aspergillus fumigatus*. *Eukaryot. Cell* 2007, *6*, 1552–1561.

[5] Lynch, A. S., Robertson, G. T., Bacterial and fungal biofilm infections. *Annu. Rev. Med.* 2008, *59*, 415–428.

[6] Blankenship, J. R., Mitchell, A. P., How to build a biofilm: a fungal perspective. *Curr. Opin. Microbiol.* 2006, *9*, 588–594.

[7] Beauvais, A., Schmidt, C., Guadagnini, S., Roux, P. *et al.*, An extracellular matrix glues together the aerial-grown hyphae of *Aspergillus fumigatus*. *Cell. Microbiol.* 2007, *9*, 1588–1600.

[8] Mowat, E., Butcher, J., Lang, S., Williams, C., Ramage, G., Development of a simple model for studying the effects of antifungal agents on multicellular communities of *Aspergillus fumigatus*. *J. Med. Microbiol.* 2007, *56*, 1205–1212.

[9] Seidler, M. J., Salvenmoser, S., Muller, F. M., *Aspergillus fumigatus* forms biofilms with reduced antifungal drug susceptibility on bronchial epithelial cells. *Antimicrob. Agents Chemother.* 2008, *52*, 4130–4136.

[10] Loussert, C., Schmitt, C., Prevost, M. C., Balloy, V. *et al.*, *In vivo* biofilm composition of *Aspergillus fumigatus*. *Cell. Microbiol.* 2009, *12*, 405–410.

[11] Carpentier, S. C., Witters, E., Laukens, K., Deckers, P. *et al.*, Preparation of protein extracts from recalcitrant plant tissues: an evaluation of different methods for two-dimensional gel electrophoresis analysis. *Proteomics* 2005, *5*, 2497–2507.

[12] Lessing, F., Kniemeyer, O., Wozniok, I., Loeffler, J. *et al.*, The *Aspergillus fumigatus* transcriptional regulator AfYap1 represents the major regulator for defense against reactive oxygen intermediates but is dispensable for pathogenicity in an intranasal mouse infection model. *Eukaryot. Cell* 2007, *6*, 2290–2302.

[13] Kniemeyer, O., Lessing, F., Scheibner, O., Hertweck, C., Brakhage, A. A., Optimisation of a 2-D gel electrophoresis protocol for the human-pathogenic fungus *Aspergillus fumigatus*. *Curr. Genet.* 2006, *49*, 178–189.

[14] Neuhoff, V., Arold, N., Taube, D., Ehrhardt, W., Improved staining of proteins in polyacrylamide gels including isoelectric focusing gels with clear background at nanogram sensitivity using Coomassie Brilliant Blue G-250 and R-250. *Electrophoresis* 1988, *9*, 255–262.

[15] Lamanda, A., Zahn, A., Roder, D., Langen, H., Improved Ruthenium II tris (bathophenantroline disulfonate) staining and destaining protocol for a better signal-to-background ratio and improved baseline resolution. *Proteomics* 2004, *4*, 599–608.

[16] Albrecht, D., Kniemeyer, O., Brakhage, A. A., Guthke, R., Normalisation of 2D DIGE data-on the way to a standard operating procedure. *BIRD'08 Schriftenreihe Informatik* 2008, *26*, 55–64.

[17] Vodisch, M., Albrecht, D., Lessing, F., Schmidt, A. D. *et al.*, Two-dimensional proteome reference maps for the human pathogenic filamentous fungus *Aspergillus fumigatus*. *Proteomics* 2009, *9*, 1407–1415.

[18] Villena, G. K., Venkatesh, L., Yamazaki, A., Tsuyumu, S., Gutiérrez-Correa, M., Initial intracellular proteome profile of *Aspergillus niger* biofilms. *Rev. Peru. Biol.* 2009, *16*, 101–108.

[19] Ruepp, A., Zollner, A., Maier, D., Albermann, K. *et al.*, The FunCat, a functional annotation scheme for systematic classification of proteins from whole genomes. *Nucleic Acids Res.* 2004, *32*, 5539–5545.

[20] Chow, C. M., RajBhandary, U. L., Developmental regulation of the gene for formate dehydrogenase in *Neurospora crassa*. *J. Bacteriol.* 1993, *175*, 3703–3709.

[21] Saleeba, J. A., Cobbett, C. S., Hynes, M. J., Characterization of the *amdA*-regulated *aciA* gene of *Aspergillus nidulans*. *Mol. Gen. Genet.* 1992, *235*, 349–358.

[22] Suzuki, K., Itai, R., Suzuki, K., Nakanishi, H. *et al.*, Formate dehydrogenase, an enzyme of anaerobic metabolism, is induced by iron deficiency in barley roots. *Plant Physiol.* 1998, *116*, 725–732.

[23] Hourton-Cabassa, C., Ambard-Bretteville, F., Moreau, F., Davy de Virville, J. *et al.*, Stress induction of mitochondrial formate dehydrogenase in potato leaves. *Plant Physiol.* 1998, *116*, 627–635.

[24] Nobile, C. J., Nett, J. E., Hernday, A. D., Homann, O. R. *et al.*, Biofilm matrix regulation by *Candida albicans* Zap1. *PLoS Biol.* 2009, *7*, e1000133.

[25] Yeater, K. M., Chandra, J., Cheng, G., Mukherjee, P. K. *et al.*, Temporal analysis of *Candida albicans* gene expression during biofilm development. *Microbiology* 2007, *153*, 2373–2385.

[26] Murillo, L. A., Newport, G., Lan, C. Y., Habelitz, S. *et al.*, Genome-wide transcription profiling of the early phase of biofilm formation by *Candida albicans*. *Eukaryot. Cell* 2005, *4*, 1562–1573.

[27] Garcia-Sanchez, S., Aubert, S., Iraqui, I., Janbon, G. *et al.*, *Candida albicans* biofilms: a developmental state associated with specific and stable gene expression patterns. *Eukaryot. Cell* 2004, *3*, 536–545.

[28] Thomas, D. P., Bachmann, S. P., Lopez-Ribot, J. L., Proteomics for the analysis of the *Candida albicans* biofilm lifestyle. *Proteomics* 2006, *6*, 5795–5804.

[29] Holdom, M. D., Lechenne, B., Hay, R. J., Hamilton, A. J., Monod, M., Production and characterization of recombinant *Aspergillus fumigatus* Cu,Zn superoxide dismutase and its recognition by immune human sera. *J. Clin. Microbiol.* 2000, *38*, 558–562.

[30] Aimanianda, V., Bayry, J., Bozza, S., Kniemeyer, O. *et al.*, Surface hydrophobin prevents immune recognition of airborne fungal spores. *Nature* 2009, *460*, 1117–1121.

[31] Baillie, G. S., Douglas, L. J., Role of dimorphism in the development of *Candida albicans* biofilms. *J. Med. Microbiol.* 1999, *48*, 671–679.

[32] Rocha, E. M., Gardiner, R. E., Park, S., Martinez-Rossi, N. M., Perlin, D. S., A Phe389Leu substitution in *ergA* confers terbinafine resistance in *Aspergillus fumigatus*. *Antimicrob. Agents Chemother.* 2006, *50*, 2533–2536.

[33] Fedorova, N. D., Khaldi, N., Joardar, V. S., Maiti, R. *et al.*, Genomic islands in the pathogenic filamentous fungus *Aspergillus fumigatus*. *PLoS Genet.* 2008, *4*, e1000046.

[34] Hof, H., Kupfahl, C., Gliotoxin in *Aspergillus fumigatus*: an example that mycotoxins are potential virulence factors. *Mycotox. Res.* 2009, *25*, 123–131.

[35] Albrecht, D., Guthke, R., Brakhage, A. A., Kniemeyer, O., Integrative analysis of the heat shock response in *Aspergillus fumigatus*. *Biomed. Chromatogr. Genomics* 2010, *11*, 32.

[36] Greenbaum, D., Colangelo, C., Williams, K., Gerstein, M., Comparing protein abundance and mRNA expression levels on a genomic scale. *Genome Biol.* 2003, *4*, 117.

[37] Wang, Y., Barbacioru, C., Hyland, F., Xiao, W. *et al.*, Large scale real-time PCR validation on gene expression measurements from two commercial long-oligonucleotide microarrays. *Biomed. Chromatogr. Genomics* 2006, *7*, 59.

[38] Kupfahl, C., Heinekamp, T., Geginat, G., Ruppert, T. *et al.*, Deletion of the *gliP* gene of *Aspergillus fumigatus* results in loss of gliotoxin production but has no effect on virulence of the fungus in a low-dose mouse infection model. *Mol. Microbiol.* 2006, *62*, 292–302.

[39] McDonagh, A., Fedorova, N. D., Crabtree, J., Yu, Y. *et al.*, Sub-telomere directed gene expression during initiation of invasive aspergillosis. *PLoS Pathog.* 2008, *4*, e1000154.

[40] Kwon-Chung, K. J., Sugui, J. A., What do we know about the role of gliotoxin in the pathobiology of *Aspergillus fumigatus*? *Med. Mycol.* 2009, *47*, S97–S103.

[41] Pihet, M., Carrere, J., Cimon, B., Chabasse, D. *et al.*, Occurrence and relevance of filamentous fungi in respiratory secretions of patients with cystic fibrosis - a review. *Med. Mycol.* 2008, *47*, 387–397.

